

Final Version - JBME Manuscript 98-055
Robust Optimization of Total Joint Replacements
Incorporating Environmental Variables

Paul B. Chang, *Brian J. Williams, *Thomas J. Santner, *William I. Notz, and Donald L. Bartel

Sibley School of Mechanical and Aerospace Engineering
Cornell University
Ithaca, New York, U.S.A.

and

*Department of Statistics
The Ohio State University
Columbus, Ohio, U.S.A.

Submitted to: Journal of Biomechanical Engineering

Running Title: Robust Optimization of Total Joint Replacements

Address correspondence to:

Paul B. Chang

222 Upson Hall, Cornell University

Ithaca NY 14853

607-255-3575

Fax: 607-255-1222

Email: pc10@cornell.edu

Nomenclature

- b = bullet tip length
- \mathbf{c} = vector of linear predictor coefficients
- d = midstem diameter
- D = implant toggling measure
- E = cancellous bone elastic modulus
- \mathbf{f} = vector of regression functions
- g = joint probability distribution for environmental variables
- L = objective function
- \hat{L} = predicted objective function
- R = correlation function
- S = normalized bone remodeling signal
- S_f = fatigue strength of implant material
- U = strain energy density
- U_o = strain energy density, intact femur
- w = competing objective weighting factor
- \mathbf{x} = design and environmental variable vector ($\mathbf{x}_d, \mathbf{x}_e$)
- \mathbf{x}_d = design variable vector (b, d)
- \mathbf{x}_e = environmental variable vector (E, \dots)
- Y = structural response
- \hat{Y} = predicted structural response
- Z = Gaussian stochastic process
- β = vector of regression coefficients (Greek l.c. beta)
- η = bone location weighting factor (Greek l.c. eta)
- θ, p = correlation parameters (Greek l.c. theta)
- θ = joint force angular deviation (Greek u.c. theta)
- σ_s = implant stress (Greek l.c. sigma)
- σ_z^2 = stochastic process variance
- ϕ = bone or implant slope (Greek l.c. phi)
- ϕ_o = maximum bone or implant slope

Summary

Direct search techniques for the optimal design of biomechanical devices are computationally intensive requiring many iterations before converging to a global solution. This along with the incorporation of environmental variables such as multiple loading conditions and bone properties make direct search techniques infeasible. In this study, we introduced new methods that are based on the statistical design and analysis of computer experiments to efficiently account for environmental variables. Using data collected at a relatively small set of training sites, the method employs a computationally inexpensive predictor of the structural response that is statistically motivated. By using this predictor in place of the simulator (e.g. finite element model), a sufficient number of iterations can be performed to facilitate the optimization of the complex system.

The applicability of these methods was demonstrated through the design of a femoral component for total hip arthroplasty incorporating variations in joint force orientation and cancellous bone properties. Beams on elastic foundation (BOEF) finite element models were developed to simulate the structural response. These simple models were chosen for their short computation time. This allowed us to represent the actual structural response surface by an exhaustive enumeration of the design and environmental variable space, and provided a means by which to validate the statistical predictor. We were able to accurately predict the structural response and the optimal design using only sixteen runs of the computer code. The general trends predicted by the BOEF models were in agreement with previous three-dimensional finite element computer simulations, and experimental and clinical results, which demonstrated that the important features of intramedullary fixation systems were captured. These results indicate that the statistically based optimization methods are appropriate for optimization studies using computationally demanding models.

Introduction

For more than two decades, computer modeling of total joint replacements has matured as a supplement to physical experiments and clinical studies. The utility of any model depends on both its fidelity to “reality” and control over the physical modeling parameters. While clinical studies offer the best representation of a patient population, they offer little control over the influential design and environmental factors. At the other end of the spectrum, computer models are furthest removed from reality, but are easily controlled. A controlled experiment is essential for isolating the effects of factors, and as such, computer experiments are ideal for design comparisons and optimization.

While the idea of computer aided design of total joint replacements is an appealing one, logistical barriers still exist. Even with today’s fastest computers, simulations can take several hours or days to perform. This can be particularly restrictive for optimization studies that require an extensive search over the space of possible design combinations. Standard iterative search algorithms have difficulties that may inhibit or prohibit their use. The most serious of these is their highly iterative nature which requires several evaluations (computer simulations) of candidate designs before converging to an optimal solution. This problem is compounded by convergence problems and the possibility of being trapped in local optima. These restrictions have been apparent in previous optimization studies that used simplified geometry (Yong et al., 1989, Huiskes and Boeklagen, 1989, de Beus et al., 1990) and a limited set of bone properties and loading conditions (Kuiper, 1993, Davy and Katoozian, 1994).

Huiskes and Boeklagen (1989) pointed out an important limitation of their study: an optimal design is only optimal with respect to the particular loading conditions under which it was determined. A hip implant, for example, may be optimized for gait loads, yet may not be stable under the large torsional moments experienced while ascending stairs (Burke et al., 1991, Kotzar et al., 1995). Similarly, bone geometry, material properties, surgical technique, and other environmental factors can affect the ultimate choice of implant design. In fact, Herberts and Malchau (1997) found that surgical technique was the most important factor influencing the risk of aseptic

loosening for total hip arthroplasty. Loading, bone properties, and surgical technique, however, cannot be explicitly controlled in the design. That is, we cannot ask a patient to walk only on level surfaces, nor can we control bone quality or surgical expertise. Instead, designs are preferred that perform favorably for a wide range of environmental conditions. Such designs are referred to as robust. “Robust optimization” is the process of determining the most robust design.

Optimizing an implant with respect to a distribution of environmental conditions requires significantly more computation than optimizing with respect to fixed environmental inputs. Therefore, the computational considerations become more important and alternatives to the traditional methods of optimization must be considered. In this paper, we introduce an efficient alternative to iterative search algorithms based on the statistical design and analysis of computer experiments (Sacks et al., 1989). The method employs an inexpensive statistical predictor of the structural response as a function of both the design and environmental variables based on calculation of the structural response at a relatively small set of variable input (training) sites. By using an *analytical* statistical predictor as a surrogate for the more expensive *numerical* simulator (e.g. a finite element model), structural responses at other sites can be quickly evaluated thereby facilitating the search for an optimal design. In fact, the method is so economical that complex three dimensional computer models can be used and evaluated for a comprehensive set of environmental conditions. While this method is new to biomechanical applications, its effectiveness has been documented in a diverse range of studies from thermal energy storage devices (Currin et al., 1991) to integrated circuit design (Bernardo et al., 1992).

We demonstrated the applicability of the statistical methods through the optimization of a femoral component for total hip arthroplasty. The structural response was predicted using one-dimensional beams on elastic foundation (BOEF) models (Hetenyi, 1946, Huiskes, 1980) with respect to an idealized distribution of joint force directions and cancellous bone properties. Simple structural models were used for two reasons. First, the structural response of flexible implants has been studied in the past (e.g. Huiskes et al., 1992, Kuiper, 1993) and can be used for comparison. Second, the short solution times of the simulations facilitates a representation of the actual

structural response over the entire space of possible design and environmental settings. This provides a basis for validating the accuracy of the statistical predictor. Validation of the statistical methods provides a solid foundation for their extension to more detailed three-dimensional computer models and representative environmental conditions.

Methods

Robust Optimization Formulation. Consider the structural response, Y , that depends on both design variables, \mathbf{x}_d , and environmental variables, \mathbf{x}_e . A robust optimal design comprises the combination of design variables that minimizes the response Y averaged over variations in the environmental variables. One such optimization formulation incorporates an integrated form of the structural response. Let $L(\mathbf{x}_d)$ be the expectation of $Y(\mathbf{x}_d, \mathbf{x}_e)$ with respect to the distribution of environmental variables, $\mathbf{g}(\mathbf{x}_e)$. The optimization formulation can then be summarized by,

$$\text{Minimize: } L(\mathbf{x}_d) = \int Y(\mathbf{x}_d, \mathbf{x}_e) \mathbf{g}(\mathbf{x}_e) d\mathbf{x}_e \quad (1)$$

over a suitable domain for \mathbf{x}_d .

It should be noted that each time an evaluation of $L(\mathbf{x}_d)$ is desired, $Y(\mathbf{x}_d, \mathbf{x}_e)$ must be evaluated multiple times to evaluate the integral. Traditional iterative search algorithms require multiple evaluations of $L(\mathbf{x}_d)$ and hence, considerably more evaluations of $Y(\mathbf{x}_d, \mathbf{x}_e)$. Remembering that each evaluation of $Y(\mathbf{x}_d, \mathbf{x}_e)$ requires a time consuming computer simulation, the solution of Equation 1 can be impractical using traditional search techniques. The next section describes an alternative, more efficient procedure.

Optimal Search Procedure. The basis of the method (Figure 1) is akin to “curve-fitting” where we determine an inexpensive statistical predictor of the true response $Y(\mathbf{x}_d, \mathbf{x}_e)$ based on the computed response at a small set of input variable (training) sites. Once the analytical predictor, $\hat{Y}(\mathbf{x}_d, \mathbf{x}_e)$, is determined, the expensive numerical computer simulations are no longer needed. The predicted objective function, $\hat{L}(\mathbf{x}_d)$, can then be quickly determined through integration of $\hat{Y}(\mathbf{x}_d, \mathbf{x}_e)$ with respect to $\mathbf{g}(\mathbf{x}_e)$ and an optimal solution sought using any number of

search techniques.

The effectiveness of the search procedure depends on the accuracy of the statistical predictor, which is in turn a function of the training sites. Intuitively, we want to select training sites $(x_i = (x_{di}, x_{ei}), i = 1, \dots, n)$ that are in some sense representative of the entire space. This ensures that no point in the space is too far from where the structural response is observed, which in turn should lead to statistical predictors that perform well over the entire space. Latin hypercube sampling (LHS) (McKay et al., 1979) is an effective procedure for uniformly distributing training sites throughout the space $\mathbf{x} = (\mathbf{x}_d, \mathbf{x}_e)$ (for more detail see Appendix A). There are many possible LHS designs for a given experiment. We chose LHS designs that maximize a function of the pairwise training site differences. The default function employed by the Algorithms for the Construction of Experimental Designs (ACED) design software was used for this purpose (Welch, 1985).

Once the training sites are chosen and the observations, \mathbf{Y} , are made at these sites, a response surface form is assumed for $Y(\mathbf{x})$, and is used as the basis for computing the Best Linear Unbiased Predictor (BLUP), $\hat{Y}(\mathbf{x})$. The BLUP minimizes the error between the estimated surface, $\hat{Y}(\mathbf{x})$, and the actual surface $Y(\mathbf{x})$ in the sense described below.

Consider the general form for a linear predictor,

$$\hat{Y}(\mathbf{x}) = \mathbf{c}^T(\mathbf{x})\mathbf{Y} \quad (2)$$

based on observations, \mathbf{Y} , computed at the training sites. We want to determine the vector $\mathbf{c}(\mathbf{x})$ that minimizes the mean square error (MSE) between the estimated surface given in Equation 2 and the actual but unknown surface $Y(\mathbf{x})$, i.e.,

$$\text{Minimize: } \text{MSE}[\hat{Y}(\mathbf{x})] = \text{E}[\mathbf{c}^T(\mathbf{x})\mathbf{Y} - Y(\mathbf{x})]^2 \quad (3)$$

and constrains the estimator to be an unbiased,

$$\text{E}[\mathbf{c}^T(\mathbf{x})\mathbf{Y}] = \text{E}[Y(\mathbf{x})] \quad (4)$$

where E is the expectation operator. This is a constrained optimization problem.

The model adopted for the response is,

$$Y(\mathbf{x}) = \mathbf{f}^T(\mathbf{x}) + Z(\mathbf{x}) \quad (5)$$

In this model the unknown response surface is viewed as a realization of a stochastic process (Sacks et al., 1989). The regression term $\mathbf{f}^T(\mathbf{x})$ (trend) models the global behavior of the response. The regression coefficient is unknown. The second term, $Z(\mathbf{x})$, is a random function (stochastic process) assumed have zero mean and covariance,

$$\text{Cov}[Z(\mathbf{w}), Z(\mathbf{x})] = E[Z(\mathbf{w})Z(\mathbf{x})] = \frac{\sigma^2}{z} R(\mathbf{w}, \mathbf{x}) \quad (6)$$

where $R(\mathbf{w}, \mathbf{x})$ is a known correlation function and $\frac{\sigma^2}{z}$ is the known or unknown stochastic process variance. It describes local deviations from the trend. In a standard regression setting, $Z(\mathbf{x})$ is a white noise uncorrelated process. In modeling computer experiments, a more complicated correlation structure is employed to account for the anticipated correlation between responses at nearby input sites. By accounting for this local variation, use of a simple trend component often suffices. Little improvement is obtained by using a more complicated trend. In many applications including the present study, only a constant is used, i.e. the vector \mathbf{f} reduces to unity. The correlation structure for Z is,

$$R(\mathbf{w}, \mathbf{x}) = \prod_{i=1}^k \exp(-\alpha_i |w_i - x_i|^{p_i}) \quad (7)$$

When \mathbf{w} and \mathbf{x} are in close proximity, the correlation between $Z(\mathbf{w})$ and $Z(\mathbf{x})$ is high. The parameters α_i ($\alpha_i > 0$) and p_i ($0 < p_i \leq 2$) for $i = 1, \dots, k$ are determined by maximum likelihood estimation. If we let \mathbf{Y} denote the $n \times 1$ vector of observed responses at the n training sites selected by LHS, then Equation 5 has the form,

$$\mathbf{Y} = \mathbf{F} + \mathbf{Z} \quad (8)$$

where \mathbf{F} is an $n \times k$ matrix of regression functions evaluated at the training sites, and \mathbf{Z} is an

$n \times 1$ random vector having mean $\mathbf{0}$ and variance-covariance matrix $\frac{2}{Z}\mathbf{R}$ where \mathbf{R} is the $n \times n$ matrix of correlations between the observed responses obtained from Equation 7.

We can now derive an expression for the MSE, and formulate the constrained optimization problem following Equations 3 and 4. The result is,

$$\text{Minimize: } \text{MSE}[\hat{Y}(\mathbf{x})] = \frac{2}{Z}[1 + \mathbf{c}^T(\mathbf{x})\mathbf{R}\mathbf{c}(\mathbf{x}) - 2\mathbf{c}^T(\mathbf{x})\mathbf{r}(\mathbf{x})] \quad (9)$$

$$\text{Subject to: } \mathbf{F}^T \mathbf{c}(\mathbf{x}) = \mathbf{f}(\mathbf{x}) \quad (10)$$

where $\mathbf{r}(\mathbf{x})$ is the $n \times 1$ vector of correlations between the responses at the training sites and the response at the unsampled input \mathbf{x} . Introducing Lagrange multipliers, solving Equations 9 and 10 for $\mathbf{c}(\mathbf{x})$, and substituting $\mathbf{c}(\mathbf{x})$ into Equation 2, we obtain the BLUP,

$$\hat{Y}(\mathbf{x}) = \mathbf{f}^T \hat{\mathbf{a}} + \mathbf{r}^T(\mathbf{x})\mathbf{R}^{-1}(\mathbf{Y} - \mathbf{F} \hat{\mathbf{a}}) \quad (11)$$

where

$$\hat{\mathbf{a}} = (\mathbf{F}^T \mathbf{R}^{-1} \mathbf{F})^{-1} \mathbf{F}^T \mathbf{R}^{-1} \mathbf{Y} \quad (12)$$

is the generalized least squares estimator of the coefficients \mathbf{a} . If the correlation structure is known up to a vector of parameters, e.g. if Equation 7 is assumed and Z is Gaussian, an Empirical BLUP (EBLUP) is obtained by substituting the maximum likelihood estimates of the unknown correlation parameters into Equation 11. It provides an estimate of the true surface, $Y(\mathbf{x})$, based on observations, \mathbf{Y} , at the training sites selected using LHS. Equation 11 can now be substituted into Equation 1 to generate an objective function predictor, $\hat{L}(\mathbf{x}_d)$. From this predictor an optimal solution can be quickly determined using traditional optimal search techniques as computational time is no longer an issue.

Example Problem. We applied the general procedure to the optimal design of a femoral component for total hip arthroplasty. Specifically, we explored the trade-offs between competing design goals arising from the use of more flexible intramedullary stems. On the one hand, a flexible implant shares more load with the periprosthetic bone thereby limiting stress shielding and

subsequent bone resorption (Engh et al., 1988, Engh et al., 1992, Bobyn et al., 1992, Sumner et al., 1991). On the other hand, a more flexible implant causes higher interface stresses and greater relative motions proximally (Huiskes et al., 1992, Kuiper, 1993). In the unbonded case, increased motion may inhibit bone ingrowth (Pilliar et al., 1986, Karrholm et al., 1992) and in the bonded case, high interface stresses may disrupt fixation.

We considered varying the cross sectional geometry of the implant to reduce stiffness. This concept has been previously realized in the Omniflex[®] design (Osteonics, Allendale NJ). It performed well relative to cemented hip implants but slightly worse than its full-sized counterpart (Omnifit) in trials performed by the same surgeon (Capello et al., 1994). Although computer simulations predicted a 40% reduction in bone loss (Huiskes et al., 1995), the stability of the Omniflex may have been compromised by the reduction in cross sectional area (Capello et al., 1994). As a result we altered only the distal portion of the implant to increase flexibility.

The design concept (Figure 2) was characterized by two design factors: a reduced midstem diameter, d , and a bullet tip length, b . Two environmental factors were also considered that contribute to the overall structural response: joint force angle () and cancellous bone elastic modulus (E). The joint force angle was measured from a neutral or average joint force angle as determined in telemetric hip force studies (Kotzar et al., 1995) and thus described deviations from an expected joint force angle. The frequency of the (E_i, θ_j) combinations were described by a discrete joint probability distribution, g_{ij} , to reflect in vivo variations (Figure 2).

The structural response, Y , was a linear combination of two competing responses,

$$Y = wS + (1 - w)D \quad (13)$$

where w was a weighting factor ranging between zero ($Y = D$) and one ($Y = S$).

S was the absolute value of a normalized bone remodeling signal (Huiskes et al., 1992) defined as the difference in strain energy density at location i in the intact femur (U_{oi}) and femur with implant (U_i), normalized by U_{oi} ,

$$S = \sum_{i=1}^n |U_{oi} - U_i| / U_{oi} = \sum_{i=1}^n |1 - U_i / U_{oi}| \quad (14)$$

where n was the total number of measurement sites in the bone and w_i was a weighting factor for location i . Strain energy density was measured on the bone surface along the periprosthetic medial and lateral aspects and each measurement site was weighted equally. A distinction was not made between a positive or negative remodeling signal implying that both bone resorption and bone hypertrophy were undesirable, although only the former was observed.

D was a normalized measure of implant rotation in the frontal plane (“toggle”) defined as,

$$D = \frac{\max_{i=1, \dots, m} (s_i - b_i)}{\max_{i=1, \dots, m} (s_{o,i} - b_{o,i})} \quad (15)$$

where m was the total number of measurement sites and s was the slope of the bone (b) or implant stem (s) in the anterior-posterior plane. The relative slope shown in the numerator was normalized by the relative slope of the worst-case condition (denominator), denoted with a subscript o . The worst case (maximum relative slope) was achieved by completely removing the distal portion of the implant. Measurement of implant toggling (D) was made in the proximal wedged region of the implant denoted by lines around the implant in Figure 2.

Referring to Equation 1, the optimization formulation was,

$$\text{Minimize: } L(b, d) = \sum_{i,j} Y(b, d, E_{ij}) g_{ij} \quad (16)$$

The optimal value of (b, d) was checked to ensure that the implant stress (σ_s) was less than its fatigue strength (S_f),

$$\sigma_s(b, d, E_{ij}) - S_f \leq 0 \quad i, j \quad (17)$$

Bone-Implant System. The proximal implant geometry was based on a cobalt chromium ($E_{cc} = 200,000$ MPa, $S_f = 350$ MPa) Ranawat-Burstein Implant (Biomet, Inc. Warsaw IN) and the distal portion was modified to represent different combinations of the distal stem design variables (b, d) (Figure 2).

The femoral geometry and material properties were based on a composite material analog of the human femur (“sawbones,” Pacific Research Laboratories, Vashon WA) representing a

medium to large male (Figure 2). The properties of the fiber composite representing cortical bone ($E_{cort} = 18,600$ MPa) and polyurethane foam representing cancellous bone ($E = 60, 200, \text{ or } 400$ MPa), reported by Pacific Research Laboratories, were similar to those of real bone. A sawbones femur was used, instead of a cadaver femur, to provide a standard basis for comparison between different implant studies. In addition, we anticipate using these femurs in similar physical experiments.

Computer Models. Axisymmetric beams on elastic foundation (BOEF) finite element models were used to simulate the bone-implant system (Figure 3). Huiskes (1980) adapted BOEF to the analysis of intramedullary devices and this method has since been employed by other researchers for implant studies (Bechtold and Riley, 1991, O’Neil, 1987, Poddar, 1984). The implant was modeled as a beam of varying axial and flexural rigidity (EA and EI). Axial and flexural rigidities of the bone beam (cortical shell) were based on cross-sectional CT scans of the femurs (GE Spiral Scanner, “High Speed Advantage”, 1 mm slices at 3 mm increments). Pixel-based composite beam calculations were performed using the geometry determined from the CT-scans and the material properties reported above.

The bone and implant beams were coupled by an elastic foundation used to model the space filling cancellous bone (polyurethane foam). Transverse and axial stiffness properties (C_r, C_a) were based on equations developed by Huiskes (1980) with modifications to account for the “wedging” effect caused by the proximal implant taper. In the distal region of the implant where foam was not present, the elastic foundation was assigned properties of cortical bone (epoxy). Two interface conditions can be modeled, zero friction and perfectly bonded. We assumed that the true frictional interface condition lies somewhere between these two extremes and calculated an average response. Structural properties for implant, bone, and foundation are shown in Figure 3 for a sample implant configuration ($b = 25$ mm, $d = 10$ mm).

The bone was constrained distally (zero deflection, zero slope), 90 mm distal to the implant tip, and the distal implant stem was unconstrained. The nominal load acting on the femoral head (Table 1) was based on in vivo telemetric hip force measurements (Kotzar et al., 1995)

and the greater trochanter load was determined from a musculoskeletal model of a typical male patient and a muscle reduction analysis similar to Paul (1967). This loading condition represented a nominal or neutral load about which fluctuations in load angle occurred. Equivalent bending moments, transverse forces, and axial forces were applied to the most proximal portions of the beams representing the implant and bone.

The models were solved for nodal displacements, forces, and moments using the CBOEF Toolbox developed at Cornell University for use with Matlab (The Mathworks, Inc., Natick MA). Stresses and strains in the bone and implant were then derived from displacements, forces, and moments using standard finite element equations for beams.

Validation Procedure. It is important to distinguish between two types of validation, statistical and biomechanical. In this study, we were primarily concerned with validation of the statistical procedure for finding an optimal solution. That is, given a particular underlying function, does the statistical predictor provide a reasonable representation? It was also important, however, to develop biomechanical models that would provide reasonable predictions of the structural response. This second validation would ensure that the statistical procedure had been applied to a physically motivated function and would provide a basis for extension to similar intramedullary fixation systems.

The optimal search procedure, outlined above, was used to predict the structural response, $Y(b, d, E, \dots)$. Specifically, a Latin hypercube sample of sixteen training sites, determined by ACED, was used to build the EBLUP predictor, $\hat{Y}(b, d, E, \dots)$. The predicted objective function \hat{L} was then computed. The Gaussian Stochastic Process (GaSP) software¹ was used to perform these calculations. To validate the statistical procedure, the predicted objective, determined using sixteen training runs of the BOEF code, was compared with the actual response surface, L , determined by computing the response at a fine grid of sites [384 combinations of (b, d, E, \dots)]. The comparison criteria were objective function value, gradient direction, and gradient magnitude.

1. GaSP was developed by Professor W. J. Welch, Department of Statistics and Actuarial Sciences, University of Waterloo, Ontario Canada.

The general trends predicted by the BOEF models were compared to previous computer studies, and experimental and clinical results.

Results

The predicted objective (Figure 4 top row) showed excellent agreement with the actual objective (Figure 4 bottom row). Contours of the predicted objective based on the 16 computer simulations and the actual objective, L , based on an exhaustive enumeration of the design and environmental variables are presented for five cases ranging from $w = 0$ (toggle priority) to $w = 1$ (bone remodelling signal priority). In each case, the gradients were similar in direction and magnitude and the predicted optima were consistent.

Implant toggling ($Y = D$) was minimized when both the bullet tip length and midstem diameter were at their maximal values (b_{max}, d_{max}) (Figure 4, $w = 0$). The bone remodeling signal ($Y = S$) was minimized when both the bullet tip length and midstem diameter were at their minimum values (b_{min}, d_{min}) (Figure 4, $w = 1$). Less intuitive, however, was the manner in which the two competing objectives interacted. The toggling response (D) dominated the bone remodelling signal, $Y = wS + (1 - w)D$, for intermediate values of w . For example, when implant toggling and bone remodelling responses were equally weighted ($w = 0.5$), the combination (b_{max}, d_{max}) still minimized the objective function.

Discussion

The statistical predictor for the structural response based on only sixteen training sites showed excellent agreement with the actual response determined by an enumeration of all combinations of design and environmental variables. It should be noted that sixteen sample runs were relatively few and second stage sampling, within a refined subspace near the first stage predicted minimum, could be performed to improve the prediction accuracy (see for example Bernardo et al., 1992). In this study, however, sixteen samples were sufficient to determine the optimal implant design.

As expected, when only the bone remodeling signal was considered in the objective, the

most flexible design was optimal. Conversely, a cylindrical stem with no reduction was optimal when only implant toggling was considered.

The predicted optimum was dependent on the value of the weighting factor in the competing objective function. Without other criteria, however, there is no single correct choice of the weighting factor and its range of values between zero and unity generates a family of optimal solutions (Bartel and Marks, 1974). This family of solutions could be presented to surgeons who would use their expertise and experience to choose an optimal design. Alternatively, a third objective could be introduced to decide on an appropriate weighting factor. Constraints may also offer a way to eliminate this uncertainty. For example, if, through clinical or experimental methods, a critical measure of implant toggling were known, it could be incorporated as a constraint rather than as a competing objective. As a result, the weighting factor would be eliminated from the objective function.

The BOEF models were relatively simple one-dimensional, linear representations of a three-dimensional nonlinear system. The statistical methods introduced are more appropriately applied to complex computer models where CPU-time is of concern. The main reason for selecting the BOEF models was for their computational efficiency which allowed for an evaluation of the structural response over all combinations of design and environmental variables. This “actual” response provided a basis for validation of the statistical procedure. The results predicted by the BOEF models, however, were consistent with previous numerical, experimental, and clinical studies cited above (Huiskes et al., 1992, Kuiper, 1993, Sumner et al., 1991, Bobyn et al., 1992, Capello et al., 1994) indicating that the simplified beams on elastic foundation models were predicting appropriate trends.

The robust optimization procedure was presented in algorithmic fashion, but it is important to realize that these methods are the focus of ongoing statistical research. For example, Latin hypercube sampling was chosen from a variety of possible sampling schemes. This class of experimental designs has two appealing features for computer experiments. First, they do not repeat values in any dimension of \mathbf{x} . This is a desirable feature for deterministic computer models

because differences arising from repeated measures (“experimental error”) do not exist. Second, a projection of an LHS design into a lower dimensional space, is also an LHS design. Not all variables initially considered have an influence on the structural response. These “inactive” variables can be easily eliminated from the analysis by considering only a subset of the initial experimental design. This projected design is guaranteed to be sufficiently space-filling, allowing the development of an accurate statistical predictor. Another example is the selection of the regression model. Traditionally, a least squares approach has been used where the response is modeled as a high-order (usually quadratic) function of all input parameters of interest. Instead, we used an alternative model that treated the deterministic response as a simple mean surface plus a draw from a Gaussian stochastic process. In preliminary studies, this model demonstrated improved accuracy compared with quadratic least squares. In addition, fewer observations are required to fit the stochastic model than are needed to fit polynomial regression models using the method of least squares.

The key feature of the proposed methodology is to replace the calculation of a complicated structural response by a much simpler predictor based on a statistical model. Thus the methodology demonstrated here can be extended to a wide variety of important biomechanical problems. For example, the robustness of the predicted optimal designs with respect to alternate distributions in the environmental variables can be examined. Temporal distributions in structural properties can be included in the analysis. For example, implants can be evaluated with respect to variations in bone properties resulting from bone remodeling, bone ingrowth, and wear-debris-initiated osteolytic processes. The effects of variations in surgical procedure and implant alignment could also be examined and compared with documented clinical results. From a mathematical analysis perspective, uncertain modeling parameters and physical quantities that are difficult or impossible to measure could be treated similarly to the environmental variables included. The only difference would be that the randomness is now motivated by uncertainty rather than by inter- or inpatient variations. As an example, interface conditions are difficult to measure directly but can have a substantial effect on the behavior of the implant (Rubin et al., 1993). A range of possible

values of interface friction could be included in an analysis by treating friction as a uniformly distributed random variable with extremes corresponding to upper and lower bounds. Finally, It is important to realize that the successful application of these methods depends on the ability to quantify distributions of interest. Many existing technologies such as computed tomography, magnetic resonance imaging, and roentgen stereophotogrammetric analysis will be particularly useful in this endeavor.

Appendix A - Latin Hypercube Sampling

Let $\mathbf{X} \in S$ be the vector of input variables. We want to determine N values of \mathbf{X} that are representative of the space S . Three methods are discussed below. The first two methods, random and stratified sampling, are described to motivate the use of the third method, Latin hypercube sampling, to determine input sites, specifically for design studies involving deterministic computer experiments.

Simple Random Sampling: A random sample of N observations is taken from the distribution of \mathbf{X} . Random sampling is susceptible to “clustering” where only certain regions of S are represented.

Stratified Sampling: To avoid clustering, S is divided into m distinct strata, $S = \{S_1, \dots, S_m\}$ where $S_i \cap S_j = \emptyset$ for $i \neq j$. A sample n_i observations is taken from the distribution of \mathbf{X} given $\mathbf{X} \in S_i$ for each stratum where, $\sum n_i = N$. Note that random sampling is a special case of stratified sampling ($m = 1$).

Latin Hypercube Sampling (LHS): The same reasoning that led to stratified sampling suggests the usefulness of stratifying on the marginal components of \mathbf{X} . Let \mathbf{X} be a vector of length k , $\mathbf{X} = (X_1, \dots, X_k)$. Each component X_i , $i = 1, \dots, k$, is divided over its range into N equal strata with marginal probability $1/N$. This results in the input space being stratified into N^k “cells.” The sampling scheme then requires N of these cells to be sampled in such a way that each marginal stratum of each component X_i is represented exactly once in the sample.

Acknowledgments

This study was supported by The Clark, Dana, and Frese Foundations, and the National Institutes of Health, Grant AR42737-01.

References

Bartel D. L., Marks R. W., 1974, "The optimum design of mechanical systems with competing design objectives," *Journal of Engineering for Industry* Vol. pp. 171-178.

Bechtold J. E., Riley D. R., 1991, "Applications of Beams on Elastic Foundation and B-Spline Solution Methodologies to Parametric Analysis of Intramedullary Implant Systems," *J Biomech* Vol. 24, pp. 441-448.

Bernardo M. C., Buck R., Liu L., Nazaret W. A., Sacks J., Welch W. J., 1992, "Integrated Circuit Design Optimization Using a Sequential Strategy," *IEEE Transaction on Computer-Aided Design* Vol. 11, pp. 361-372.

Bobyn J. D., Mortimer E. S., Glassman A. H., Engh C. A., Miller J. E., Brooks C. E., 1992, "Producing and avoiding stress shielding, laboratory and clinical observations of noncemented total hip arthroplasty," *Clin Orthop* Vol. 274, pp. 79-96.

Burke D. W., O'Connor D. O., Zalenski E. B., Jasty M., Harris W. H., 1991, "Micromotion of cemented and uncemented femoral components," *J Bone Joint Surg [Br]* Vol. 73, pp. 33-37.

Capello W. N., Sallay P. I., Feinberg J. R., 1994, "Omniflex Modular Femoral Component, two to five year results," *Clin Orthop* Vol. 298, pp. 54-59.

Currin C., Mitchell T., Ylvisaker D., 1991, "Bayesian prediction of deterministic functions, with applications to the design and analysis of computer experiments," *Journal of the American Statistical Association* Vol. 86, pp. 953-963.

Davy D. T., Katoozian H., 1994, "Three-dimensional shape optimization of femoral components of hip prostheses with frictional interfaces," *Trans Orthop Res Soc* 19, New Orleans, Louisiana.

de Beus A. M., Hoeltzel D. A., Eftekhar N. S., 1990, "Design optimization of a prosthesis stem reinforcing shell in total hip arthroplasty," *J Biomech Eng* Vol. 112, pp. 347-357.

Eng C. A., Bobyn J. D., 1988, "The influence of stem size and extent of porous coating on femoral bone resorption after primary cementless hip arthroplasty," *Clin Orthop* Vol. 231, pp. 7-28.

Eng C. A., McGovern T. F., Bobyn J. D., Harris W. H., 1992, "A quantitative evaluation of periprosthetic bone remodeling after cementless total hip arthroplasty," *J Bone Joint Surg [Am]* Vol. 74, pp. 1009-1020.

Herberts P., Malchau H., 1997, "How outcome studies have changed total hip arthroplasty practices in Sweden.," *Clin Orthop* Vol. 344, pp. 44-60.

Hetenyi M., 1946, "Beams on Elastic Foundation, Theory with Applications in the Fields of Civil and Mechanical Engineering," University of Michigan studies. Scientific Series, ed. G Cumberlege. Vol. 16. Ann Arbor, The University of Michigan Press.

Huiskes R., 1980, "Some fundamental aspects of human joint replacement," *Acta Orthop Scand* Supplement no. 185, pp.

Huiskes R., Boeklagen R., 1989, "Mathematical Shape Optimization of Hip Prosthesis Design," *J Biomech* Vol. 22, pp. 793-804.

Huiskes R., van Rietbergen B., 1995, "Preclinical testing of total hip stems. The effects of coating placement.," *Clin Orthop* Vol. 319, pp. 64-76.

Huiskes R., Weinans H., van Rietbergen B., 1992, "The Relationship Between Stress Shielding and Bone Resorption Around Total Hip Stems and the Effects of Flexible Materials," *Clin Orthop* Vol. 274, pp. 124-134.

Karrholm J., Borssen B., Lowenhielm G., Snorrason F., 1994, "Does early micromotion of femoral stem prostheses matter? 4-7 year stereoradiographic follow-up of 84 cemented prostheses.," *J Bone Joint Surg [Br]* Vol. 76, pp. 912-917.

Kotzar G. M., Davy D. T., Berilla J., Goldberg V. M., 1995, "Torsional Loads in the Early Postoperative Period Following Total Hip Replacement," *J Orthop Res* Vol. 13, pp. 945-955.

Kuiper J. H., 1993, "Numerical Optimization of Artificial Hip Joint Designs," Ph.D. Thesis, University of Nijmegen, The Netherlands.

McKay M. D., Beckman R. J., Conover W. J., 1979, "A Comparison of Three Methods for Selecting values of Input Variables in the Analysis of Output from a Computer Code," *Technometrics* Vol. 21, pp. 239-245.

O'Neil D. A., 1987, "Structural Sensitivity of Design Variables in Segmental Fixation Devices," M.S. Thesis, Cornell University, Ithaca, New York.

Paul J. P., 1967, "Forces at the Human Hip," Ph.D. Thesis, University of Glasgow, Glasgow, Scotland.

Pilliar R. M., Lee J. M., Maniopoulos C., 1986, "Observations on the effect of movement on bone ingrowth into porous-surfaced implants," *Clin Orthop* Vol. 208, pp. 108-113.

Poddar B., 1984, "Analysis and Design of Bone-Stem Composites: Beam on Elastic Foundation Theory," M.S. Thesis, Cornell University, Ithaca, New York.

Rubin P. J., Rakotomanana R. L., Leyvraz P. F., Zysset P. K., Curnier A., Heegaard J. H., 1993, "Frictional interface micromotions and anisotropic stress distribution in a femoral total hip component," *J Biomech* Vol. 26, pp. 725-739.

Sacks J., Welch W. J., Mitchell T. J., Wynn H. P., 1989, "Design and analysis of computer experiments (with discussion)," *Statistical Science* Vol. 4, pp. 409-435.

Sumner D.R., Turner T.M., Urban R.M., Galante J.O., 1991, "Experimental Studies of Bone Remodeling in Total Hip Arthroplasty," *Clin Orthop* Vol. 276, pp. 83-90.

Welch, W. J., 1985, "ACED: Algorithms for the Construction of Experimental Designs," *Amer Statist* Vol. 39, pp. 146.

Yong S. Y., Gun H. J., Young Y. K., 1989, "Shape optimal design of the stem of a cemented hip prosthesis to minimize stress concentration in the cement layer," *J Biomech* Vol. 22, pp. 1279-1284.

Figure 1. Optimal search technique. Input sites were selected using Latin hypercube sampling (LHS) based on initial definitions of design variable bounds ($\mathbf{x}_d^{min}, \mathbf{x}_d^{max}$) and environmental variable bounds ($\mathbf{x}_e^{min}, \mathbf{x}_e^{max}$). Once the input sites were chosen and evaluated using the computer simulations, a response surface form was assumed for $Y(\mathbf{x})$ based on a stochastic process model, and the Empirical Best Linear Unbiased Predictor (EBLUP) of Y was computed. The computationally inexpensive predictor was then used in place of the computer simulations to determine the predicted objective function \hat{L} and to locate the optimal design \mathbf{x}_d .

Figure 2. Hip implant design and femur model for optimization study. The proximal implant geometry was a cobalt chromium Ranawat-Burstein Implant (Biomet, Inc. Warsaw IN) and the distal portion was modified to represent different combinations of the midstem diameter (d) and bullet-tip length (b). The implant design concept does not represent a commercial device. Composite material analogs (Pacific Research Laboratories, Vashon WA) represented the left femur of an adult male. Joint force orientation, θ , was measured from a reference angle derived from telemetric joint force measurements (Kotzar et al., 1995). A medial view of a composite femur with the femoral head excised shows the polyurethane foam representing cancellous bone. The probability of each (E_i, θ_j) combination was idealized by a discrete joint probability distribution, g_{ij} , to reflect in vivo variations.

Figure 3. Structural properties for input into the coupled beams on elastic foundation (BOEF) solver for an example implant configuration ($b = 25$ mm, $d = 10$ mm). The axial and flexural rigidities (EA and EI) were generally greater for the metallic implant except in the region of the reduced midstem diameter. Axial and transverse foundation stiffnesses (C_a and C_t) were averaged between the perfectly bonded and frictionless cases as it was assumed that the true interface condition lied somewhere in between these two extremes. At the top of the figure a schematic of the BOEF model is presented with load orientations (F_x - axial force, F_y - transverse force, M_z - moment) indicated.

Figure 4. Contours of predicted surface (\hat{L}) based on 16 samples (top row) compared with contours of the actual surface (L) based on 384 samples (bottom row). The five columns represent dif-

ferent relative weighting (w) of bone remodeling signal (S) and implant toggling (D). The dark shaded regions are areas of minimum response.

Table 1: Nominal loading condition. All forces are expressed in Newtons for a 750 N patient. Two components of force are given for the two-dimensional beams on elastic foundation analysis. Refer to Figure 2 for coordinate system.

	Axial (N)	Medial (N)
Joint Contact Force	-1770	-436
Abductor Muscle Force	844	488

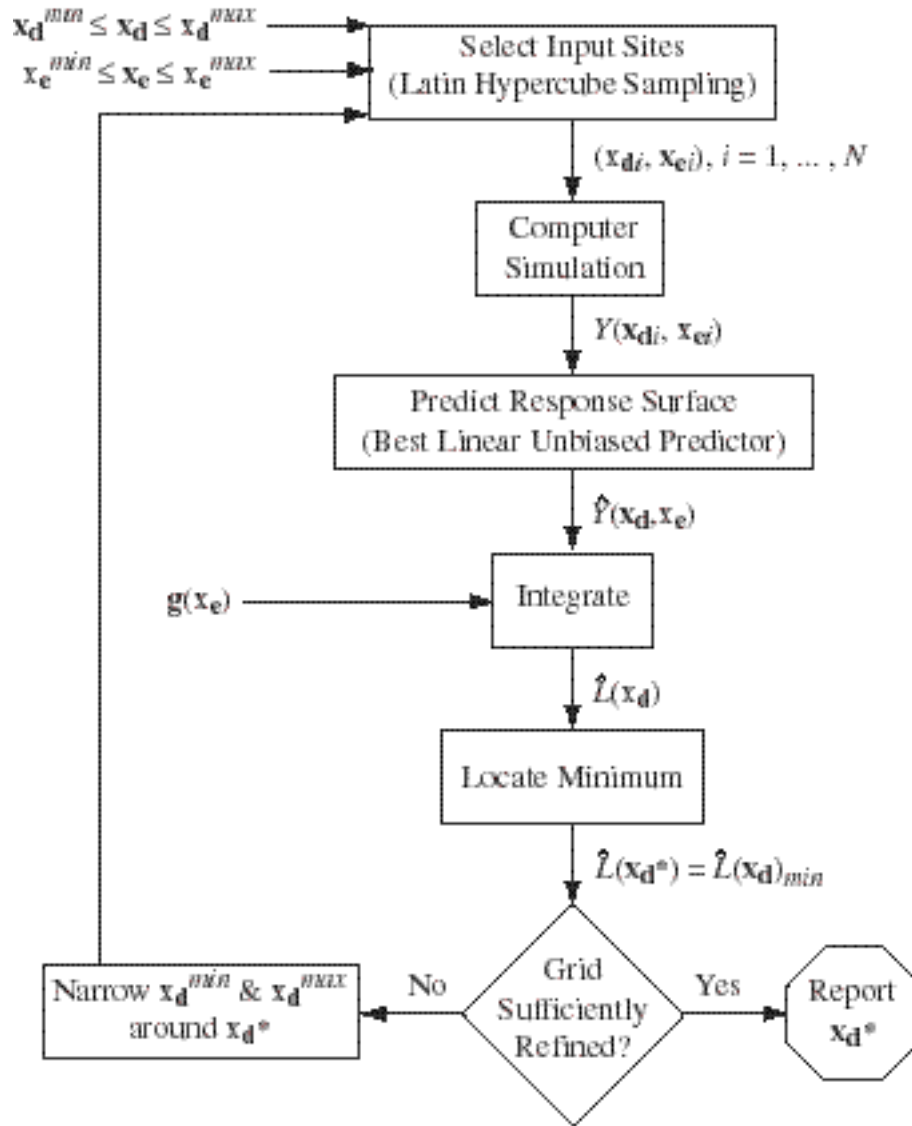


Figure 1. Optimal search technique. Input sites were selected using Latin hypercube sampling (LHS) based on initial definitions of design variable bounds (\mathbf{x}_d^{\min} , \mathbf{x}_d^{\max}) and environmental variable bounds (\mathbf{x}_e^{\min} , \mathbf{x}_e^{\max}). Once the input sites were chosen and evaluated using the computer simulations, a response surface form was assumed for $Y(\mathbf{x})$ based on a stochastic process model, and the Empirical Best Linear Unbiased Predictor (EBLUP) of Y was computed. The computationally inexpensive predictor was then used in place of the computer simulations to determine the predicted objective function \hat{L} and to locate the optimal design \mathbf{x}_d^* .

Paul B. Chang

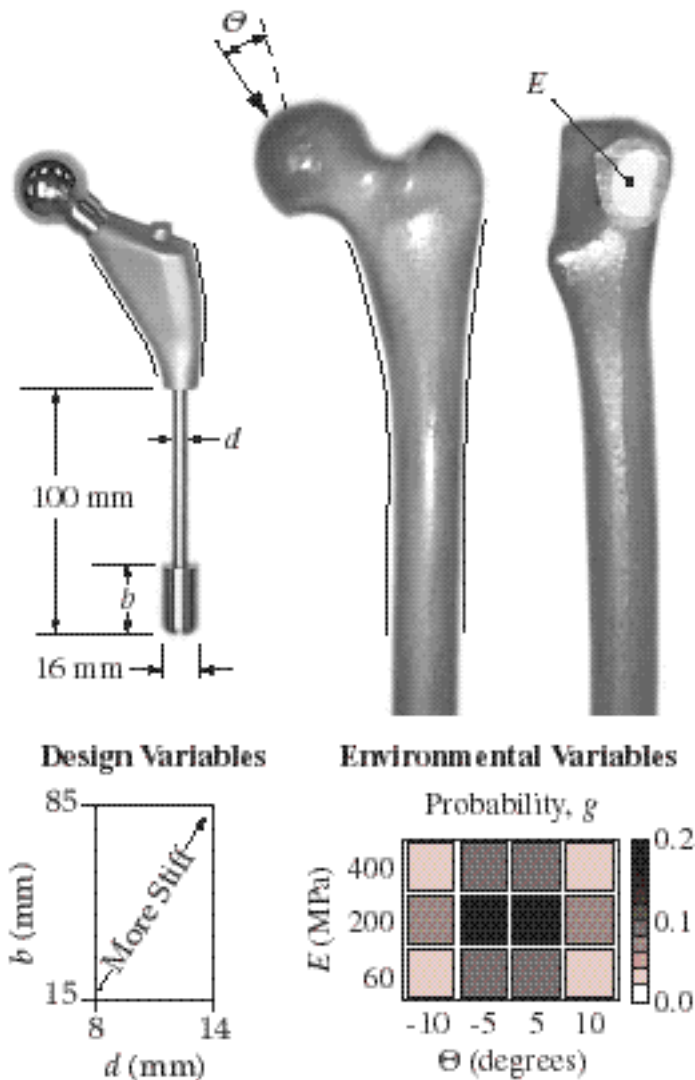


Figure 2. Hip implant design and femur model for optimization study. The proximal implant geometry was a cobalt chromium Ranawat-Burstein Implant (Biomet, Inc. Warsaw IN) and the distal portion was modified to represent different combinations of the midstem diameter (d) and bullet-tip length (b). The implant design concept does not represent a commercial device. Composite material analogs (Pacific Research Laboratories, Vashon WA) represented the left femur of an adult male. Joint force orientation, Θ , was measured from a reference angle derived from telemetric joint force measurements (Kotzar et al., 1995). A medial view of a composite femur with the femoral head excised shows the polyurethane foam representing cancellous bone. The probability of each (E_i, Θ_j) combination was idealized by a discrete joint probability distribution, g_{ij} , to reflect in vivo variations.

Paul B. Chang

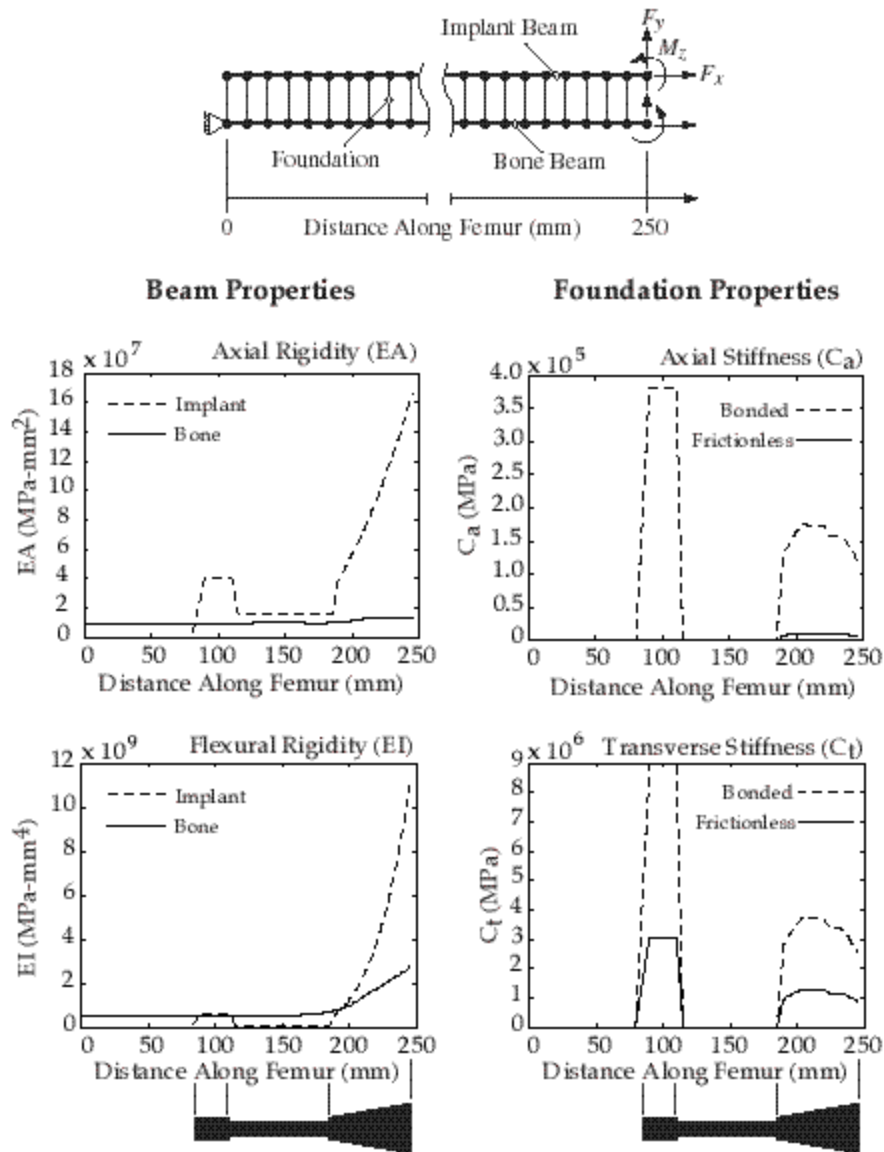


Figure 3. Structural properties for input into the coupled beams on elastic foundation (BOEF) solver for an example implant configuration ($b = 25$ mm, $d = 10$ mm). The axial and flexural rigidities (EA and EI) were generally greater for the metallic implant except in the region of the reduced midstem diameter. Axial and transverse foundation stiffnesses (C_a and C_t) were averaged between the perfectly bonded and frictionless cases as it was assumed that the true interface condition lies somewhere between these two extremes. At the top of the figure a schematic of the BOEF model is presented with load orientations (F_x - axial force, F_y - transverse force, M_z - moment) indicated.

Paul B. Chang

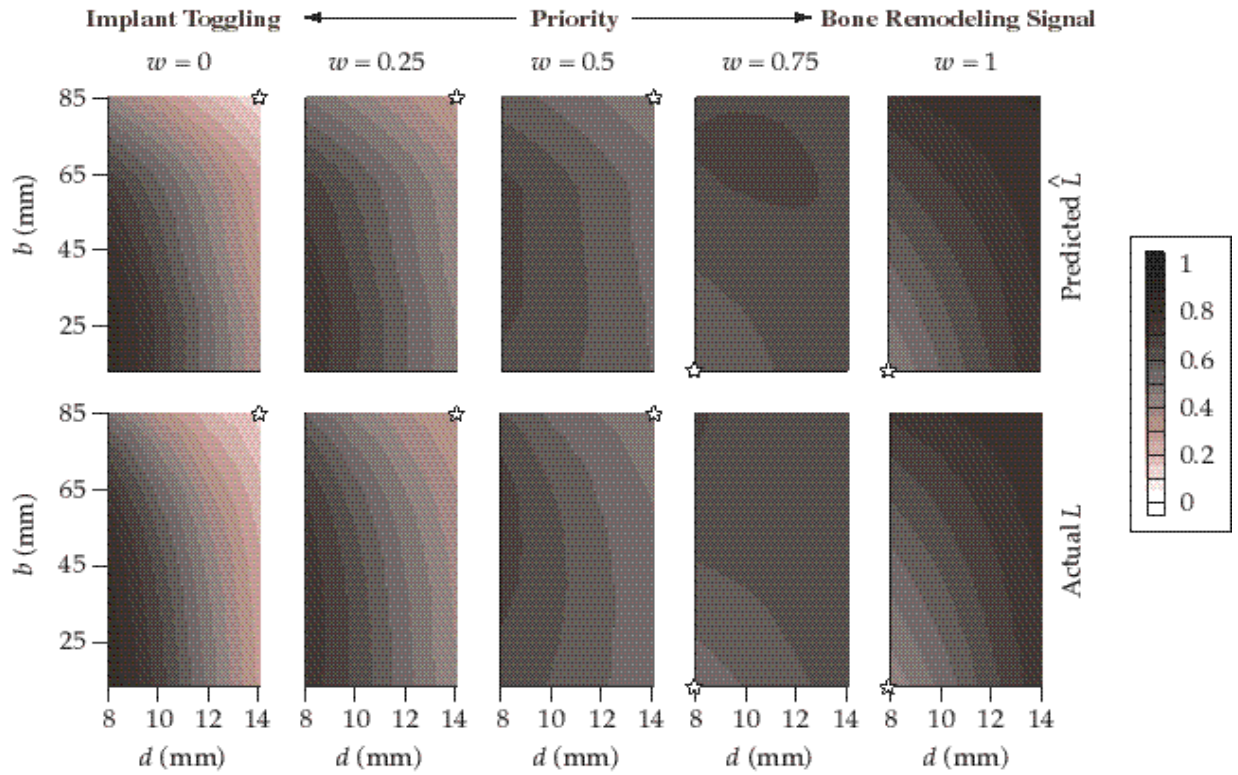


Figure 4. Contours of predicted surface (\hat{L}) based on 16 samples (top row) compared with contours of the actual surface (L) based on 384 samples (bottom row). The five columns represent different relative weighting (w) of bone remodeling signal (S) and implant toggling (D). The dark shaded regions are areas of minimum response and the stars indicate the optima for each case of w .

Paul B. Chang